Nano Energy 37 (2017) 268–274

Contents lists available at ScienceDirect

Nano Energy

journal homepage: www.elsevier.com/locate/nanoen

Full paper

Flexible PET/EVA-based piezoelectret generator for energy harvesting in harsh environments

Junwen Zhong[a,1], Qize Zhong[b,1], Xining Zang[a], Nan Wu[c], Wenbo Li[c], Yao Chu[a,d], Liwei Lin[a,d,*]

[a] Department of Mechanical Engineering, University of California at Berkeley, Berkeley, CA 94720, United States
[b] Temasek Laboratories (TL@ NTU), Nanyang Technological University, 50 Nanyang Drive, 637553 Singapore
[c] Wuhan National Laboratory for Optoelectronics, and School of Optical and Electronic Information, Huazhong University of Science and Technology, Wuhan 430074, China
[d] Sensors and Microsystems Laboratory, Tsinghua-Berkeley Shenzhen Institute, Shenzhen 518055, China

ARTICLE INFO

Keywords:
Mechanical energy
Flexible generator
Harsh environment
Piezoelectret

ABSTRACT

Stable and repeatable operation is paramount for practical and extensive applications of all energy harvesters. Herein, we develop a new type of flexible piezoelectret generator, which converts mechanical energy into electricity consistently even under harsh environments. Specifically, the generator, with piezoelectric coefficient (d_{33}) reaching ~ 6300 pC/N, had worked stably for continuous ~ 90000 cycles, and the generator pressed by a human hand produced load peak current and power up to ~ 29.6 μA and ~ 0.444 mW, respectively. Moreover, the capability to steadily produce electrical power under extreme moisture and temperature up to 70 °C had been achieved for possible applications in wearable devices and flexible electronics.

1. Introduction

With the rise of intelligent wearable electronics, energy harvesters converting ambient mechanical energy into electricity have attracted much attention, which is not only because the energy source (*e.g.* human body movement, airflow, sound vibration, water waves *etc.*) ubiquitously exists in ambient background and is free, but also because the converting energy could enable these electronics to be functional indefinitely, thereby reducing the dependence on battery power [1–3]. Recently, flexible generators based on different working mechanism mainly including piezoelectric [4,5], electromagnetic [1,6] and electrostatic effect [3,7–17] have been successfully demonstrated with typical applications in mobile health care [8,13], human-machine interaction [9,14], wireless communication [15] and self-charging cells [10,11], *etc.* Among these generators, flexible electrostatic generators like triboelectric generators [3,7–12] and electret generators [13–17], have obtained more interests due to their simple fabrication process, high conversion efficiency and environmentally friendly without chemical processing. However, the output properties and stability of those generators are mainly determined by the surface surplus charges [15,18,19], which will be neutralized, once exposed to the moist air atmosphere, impairing the output performance of generators [20–22]. Thus, well encapsulation of these electrostatic generators is required to endure long-term exposure to harsh environments. Previously, Guo et al. demonstrated a water-proof triboelectric generator that could be driven by the water flow [23], and Lee et al. had developed a fully packaged triboelectric sensors array for mapping the distribution of foot produced pressure [24]. However, the additional packaging material would add volume and reduce the flexibility of the generators [15,20]. New strategy with minimum packaging materials and low impact on the flexibility should be considered for flexible generators operating under harsh environments.

Flexible piezoelectret, known of high piezoelectric coefficient (d_{33}), light-weight and low-cost, *etc*, has extensive transducer applications, such as energy harvesters [25–28] and loudspeakers [29]. Since the electric dipole-like charges are produced inside the materials [25], the piezoelectret generators, one kind of electrostatic generators, have the potential to be excellent energy harvester candidates that still can perform well in harsh environments. In this work, we present a new type of flexible piezoelectret generator based on the polyethylene terephthalate (PET) electret film and the ethylene vinyl acetate copolymer (EVA) adhesive layer *via* a hot-pressing method. The corona charging technique was used to generate megascopic electric dipoles inside a big air bubble of the generator. Mechanical push and release the generator will change the dipole moments of the electric dipoles and alter the electrostatic induction intensity to generate alternating electricity, with d_{33} coefficient reaching ~ 6300 pC/N and stable outputs for continuous ~ 90000 operations. Experimentally, the

* Corresponding author at: Department of Mechanical Engineering, University of California at Berkeley, Berkeley, CA 94720, United States.
E-mail address: lwlin@me.berkeley.edu (L. Lin).
[1] J. W. Zhong and Q. Z. Zhong contributed equally to this work.

http://dx.doi.org/10.1016/j.nanoen.2017.05.034
Received 23 February 2017; Received in revised form 13 May 2017; Accepted 14 May 2017
Available online 17 May 2017

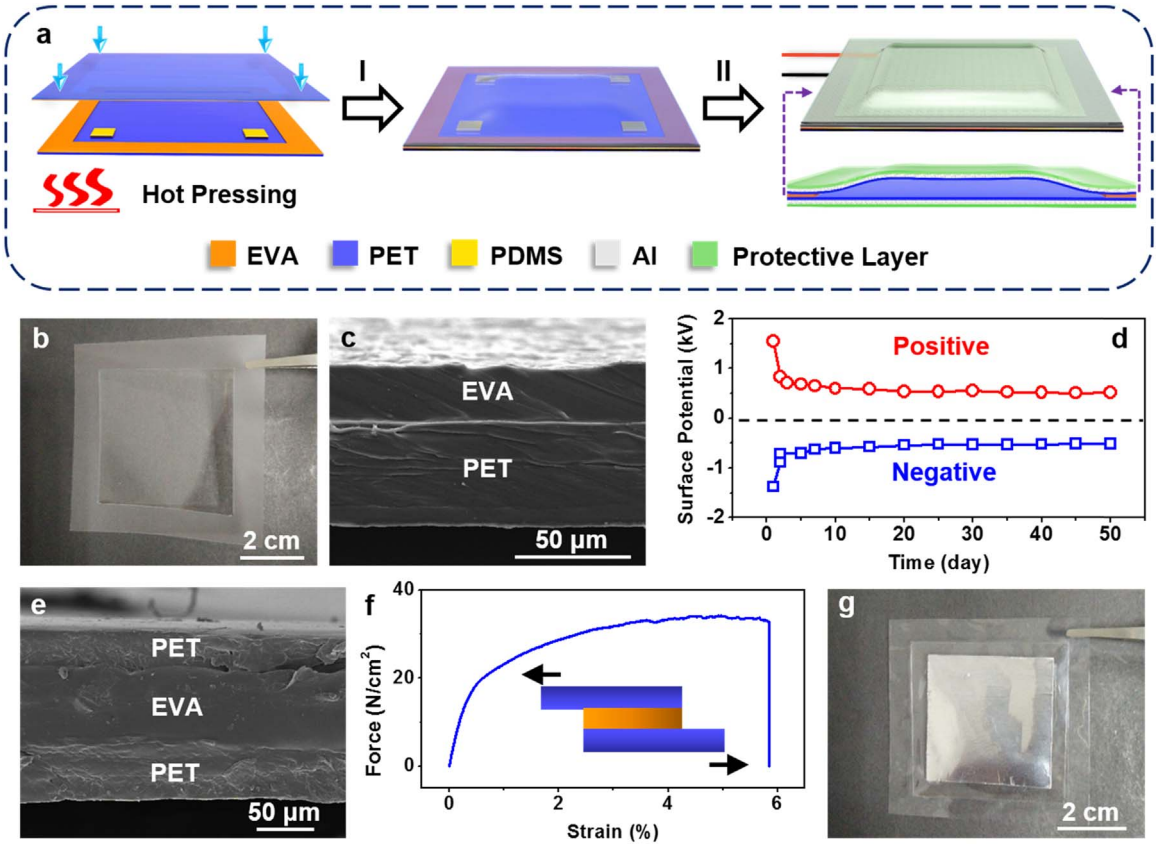

Fig. 1. Fabrication of the flexible PET/EVA-based piezoelectret generator. (a) Schematic diagram showing the fabrication steps of the generator, (I) hot pressing and corona charging; (II) placing and adhesion of the electrodes and protective layers. (b) An optical photo of the EVA/PET laminated film. (c) Cross-section view SEM image of the EVA/PET laminated film. (d) Surface potential *versus* time curves for the PET electret with positive and negative corona charging, showing little decay after the first 5 days. (e) Cross-section view SEM image of the PET/EVA/PET laminated film. (f) Mechanical shear testing result of the PET/EVA/PET laminated film. (g) An optical photo showing a fabricated generator.

generator pressed by a human hand produced load peak current and power up to ~ 29.6 μA and ~ 0.444 mW, respectively. Moreover, the most prominent advantage of this generator is the remarkable output stability under harsh environments of extreme moisture and temperature up to 70 °C, indicating that the generator may be suitable for wearable energy harvesting and used in other harsh environments.

2. Results and discussion

2.1. Fabrication of the flexible PET/EVA-based piezoelectret generator

The detailed fabrication steps of the flexible PET/EVA-based piezoelectret generator are schematically given in Fig. 1a and Fig. S1. The raw material was the flexible ~ 45 μm-thick PET electret film with the ~ 25 μm-thick and ring-shape EVA adhesive layer at the boundary, which was defined as the EVA/PET laminated film (Fig. 1**b**). The cross-section view scanning electron microscope (SEM) image (Fig. 1**c**) clearly shows the EVA/PET laminated structure. The surface morphology of the PET electret film was investigated by atomic force microscope (AFM), indicating the PET surface roughness varied from ~ −82 to ~ 78 nm (Fig. S2). In theory, the rough surface morphology is helpful to capture more surplus charges. The charges capturing ability of the PET electret film was studied *via* the corona charging method [15], as indicated in Fig. S3. In this work, two PET electret films were charged with positive and negative high voltages (values of 20 and −20 kV), respectively, and then the corresponding surface potential *versus* time curves were measured (Fig. 1**d**). It's found that the surface potential for positive and negative charging still maintained at about 0.52 and −0.50 kV after 50 days, respectively. These results indicate that the PET electret film is an excellent electret material, with the ability to capture and maintain both positive and negative surplus charges for a long time.

The fabrication steps began with fixing four polydimethylsiloxane (PDMS) spacers (size of 0.5×0.25 cm^2, thickness of 1 mm) on four corners of the EVA/PET laminated film (Fig. S1-**I and** Fig. S4a). Subsequently, another EVA/PET laminated film placed at the top was bonded to the laminated film with spacers *via* a hot-pressing method (Fig. 1-**I,** Fig. S1-**II**), forming the PET/EVA/PET laminated film with an arch-shaped air bubble with the height of 0.5–1 mm (Fig. S4b). The cross-section view SEM image indicates that the two EVA/PET laminated films were bonded tightly (Fig. 1**e**). Moreover, the PET/EVA/PET laminated film could stand the shearing force up to ~ 33 N/cm^2 before separation, indicating the strong mechanical bonding characteristics (Fig. 1**f**).

The as-fabricated PET/EVA/PET laminated film was then corona charged, in order to generate megascopic electric dipoles inside the air bubble (Fig. S1-**III**) [26]. In the next step, aluminum (Al) adhesive tape (thickness of ~ 100 μm) was covered on two outside surfaces of the charged PET/EVA/PET laminated film, as the electrodes (Fig. S1-**IV**). Lastly, two protective layers (water proof tape, thickness of ~ 50 μm) were covered on two Al electrodes (Fig. S1-**V**), forming a PET/EVA-based flexible electret generator with effective area of about ~ 4×4 cm^2 (Fig. 1-**II and** Fig. 1**g**).

2.2. Working mechanism of the PET/EVA-based flexible piezoelectret generator

By virtue of the megascopic electric dipoles inside the air bubbles, piezoelectret materials have the piezoelectric-like property as the

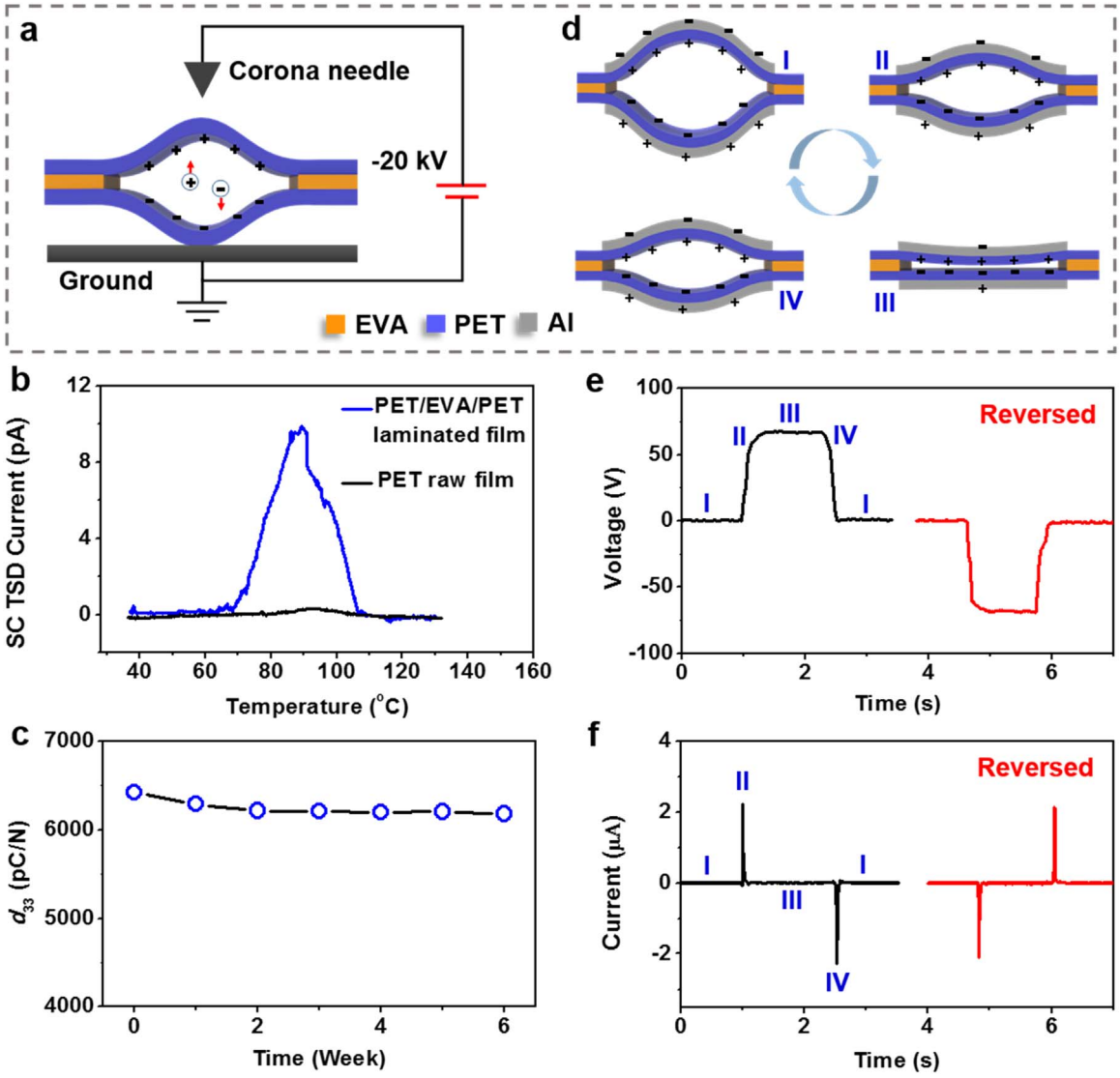

Fig. 2. Working mechanism of the flexible PET/EVA-based piezoelectret generator. (a) Schematic diagram indicating the corona charging method. (b) Short circuit TSD current measurement results for the PET/EVA/PET laminated film and PET raw film. (c) The characterized d_{33} coefficient for the generator placed in the indoor atmosphere for 6 weeks. (d) Schematic diagram indicating the electricity generation of the generator when it is at (I) original, (II) compressing, (III) equilibrium and (IV) releasing states, respectively. (e) Open-circuit voltages and (f) short-circuit currents for the generator when it was forward-connected and reverse-connected to the measurement system, respectively.

traditional piezoelectric materials, similar to lead zirconate titanate (PZT), zinc oxide (ZnO) and polyvinylidene fluoride (PVDF), *etc* [25,30,31]. Herein, the corona charging method was used to generate electric dipoles inside the air bubble of the PET/EVA/PET laminated film before the two electrodes were added on the outer surfaces, as shown in Fig. 2**a**. Specifically, high voltage up to −20 kV was applied on the corona needle for about 3 min, with samples placed about 5 cm below the needle tip. Under the strong electric field intensity, the air in the air bubble was broken down to generate ionic charges with both polarities. The positive and negative ionic charges were driven by the electric field, and captured by the upper and lower inner PET surfaces, respectively. As a result, the air bubble with charged PET inner surfaces worked as megascopic electric dipoles.

The short circuit thermally stimulated discharge (TSD) method was employed to verify the existence of electric dipoles (Fig. S5). Specifically, our laminated film and PET raw film were corona charged first, and then two outer surfaces were covered by Al electrodes. The samples were heated in a thermal chamber with a temperature rising rate of 3 °C/min, and the induced current curves were recorded *in-situ* by an electrometer. If there are electric dipoles, measurable electrical current peak in the heating process can be measured. As indicated in Fig. 2**b**, the measured current curve of the PET/EVA/PET laminated film consisted of a current peak started at about 70 °C and ended at about 110 °C, with the maximum peak value located at about 90 °C. The influences from the potential shape changes of the air bubble were negligible as no visible output currents were measured before 70 °C. In comparison, no significant current peak was observed in the short circuit TSD current curve of the PET raw electret film.

To measure the quasi-static piezoelectric d_{33} coefficient, a generator was operated by a give force F and the corresponding short-circuit output current was recorded (Fig. S6a). The value of transferred charges Q was achieved by integrating the current over time (Fig. S6b), and the d_{33} coefficient can be calculated [26]:

$$d_{33} = Q/F \tag{1}$$

The d_{33} coefficient of our generator reached ~ 6300 pC/N, which was significantly larger than that of generators based on traditional cellular polypropylene (PP) piezoelectret film (Fig. 2**c**) [26,32]. This outstanding piezoelectric property is attributed to the excellent charges capturing ability of PET electret and low elastic modulus of the air bubble structure. Moreover, the stability of d_{33} coefficient was investigated by placing the generator in indoor atmosphere for weeks and it

maintained in a narrow range around the original value for 6 weeks, as indicated in Fig. 2**c**.

Based on above piezoelectric-like behavior, Fig. 2**d** schematically illustrates the power generating processes of the generator. At any states, the megascopic electric dipoles will generate induced charges on the top and bottom Al electrodes, and the charge density on the electrode (σ_e) is decided by the following equation [27]:

$$\sigma_e = -\varepsilon_0 \varepsilon E = \frac{\varepsilon \sigma_0}{\left(\frac{D_1}{D_2} + \varepsilon\right)} \quad (2)$$

where ε_0 and ε are the dielectric constant of air and relative dielectric constant of PET, respectively. E is the electric field in the PET layer and σ_0 represents the charge density captured by the PET inner surface. D_1 is the thickness of PET layer and D_2 is thickness of air bubble or the dipole moments of the megascopic electric dipoles. In our case, ε_0, ε, E, σ_0, and D_1 are constants, and σ_e is affected by D_2.

Fig. 2**d-f** show a non-sinusoidal excitation (hand pressing motion) of the generator with the resulting open-circuit voltage response and short-circuit current response. In the original state (Fig. 2**d-I**), the electrical potential between the two electrodes are in equilibrium state, and no open-circuit voltage or short-circuit current can be observed (Fig. 2**e-I and** Fig. 2**f-I**). When the generator is compressed (Fig. 2**d-I to III,** during the very short **state II**), D_2 decreases and the charge densities on the top and bottom electrodes also decrease. The open circuit voltage curve increases in the whole compressing process (Fig. 2**e-I to III**). The short circuit current curve increases to positive peak value (Fig. 2**f-I to II**) and then drops to zero (Fig. 2**f-II to III**), resulting a sharp positive current peak. As the compression state maintains (Fig. 2**d-III**), a new equilibrium is established. The open-circuit voltage keeps at the highest value (Fig. 2**e-III**) and the short circuit current keeps at zero (Fig. 2**f-III**). It is noted that most of the surplus charges will not be neutralized when the two PET layers are contacted with each other, which is benefit by the rough surface morphology of the PET (Fig. S2). If the generator is released (Fig. 2**d-III to I,** during the very short **state IV**), D_2 increases because of the mechanical elasticity of the generator. The charge density on both electrodes will increase. The open-circuit voltage drops from highest value to zero (Fig. 2**e III to I**). The short circuit current increases to negative peak value (Fig. 2**f-III to IV**) and then drops to zero (Fig. 2**f-IV to I**), resulting a sharp negative current peak. At last, the electrical potential between the two electrodes become in equilibrium state again.

In general, the basic working mechanism of the generator is the electrostatic induction effect caused by the megascopic electric dipoles. Compressing and releasing the generator will change the dipole moments of the electric dipoles. Thus, the electrical potential between the two electrodes are changed, and the alternating electricity is generated. Switching polarity tests were also carried out to confirm that the measured output signals are generated from the generator rather than from the artifacts of the measurement system (given in the right side of Fig. 2**e and f**).

2.3. Electrical output properties of the flexible PET/EVA-based piezoelectret generator

The electrical outputs of the flexible PET/EVA-based piezoelectret generator were carefully investigated by periodically compressing and releasing at controlled pressure and sinusoidal frequency. Typically, the generator was attached to a force meter, which was tightly fixed onto an x-y-z mechanical stage.

By virtue of the large piezoelectric d_{33} coefficient, the output properties of our generator were excellent. Under given applied pressure of 6.67 kPa and sinusoidal frequency of 5 Hz, the load peak current and power density of the generator with different external

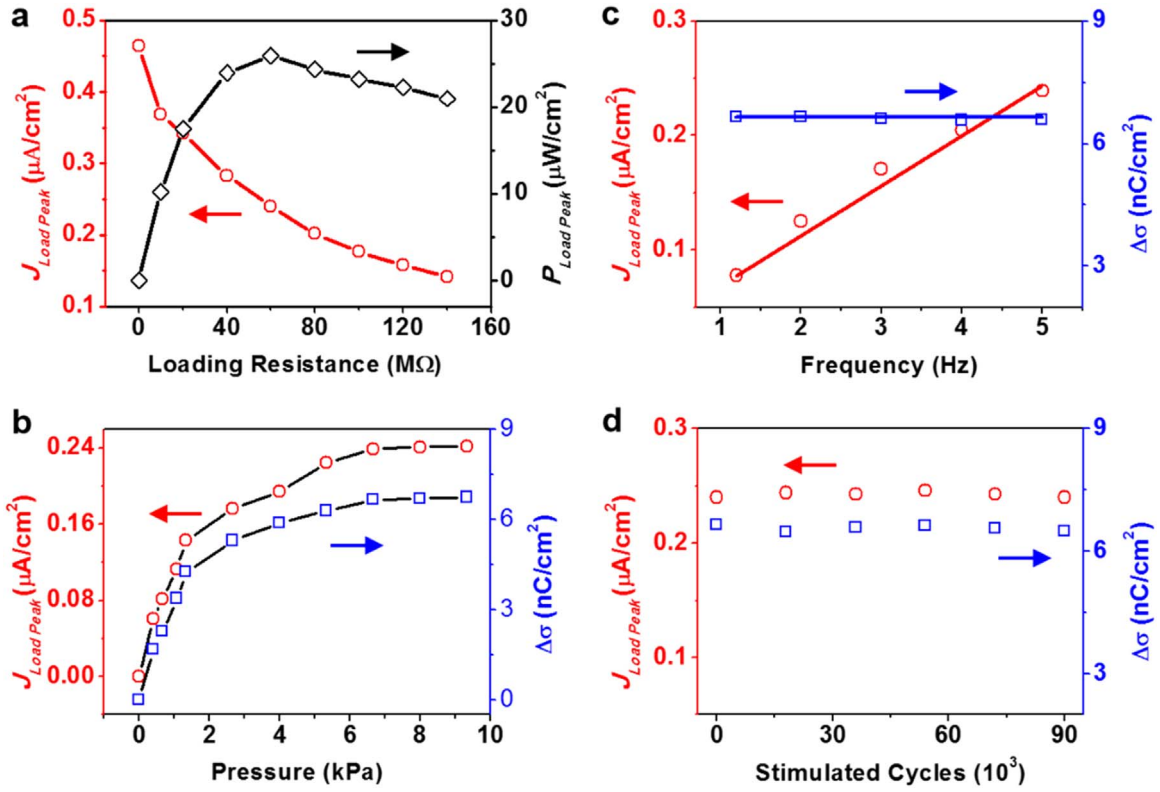

Fig. 3. Electrical outputs of the flexible PET/EVA-based piezoelectret generator. (a) Load peak current and power density of a generator with respect to different load resistances, under given applied pressure of 6.67 kPa and sinusoidal frequency of 5 Hz. (b) Load peak current and transferred charge density for a generator with respect to given applied frequency of 5 Hz and different applied pressure. (c) Load peak current and transferred charge density for a generator respect to given applied pressure of 6.67 kPa and different applied frequency. (d) Load peak current and transferred charge density for a generator for continuous operations of 90000 cycles, under given applied pressure and frequency of 6.67 kPa and 5 Hz.

resistors were measured (Fig. 3**a**). The maximum load peak power density reached ~ 25.923 μW/cm ^{2}, when the corresponding load peak current density and load resistance were ~ 0.241 μA/c m^2 and 60 MΩ, respectively. It should be noted that unless otherwise specified, the load resistance is 60 MΩ for optimal outputs for the prototype system.

The load peak current density and corresponding transferred charge density (△σ) for the generator under given applied frequency of 5 Hz and different applied pressure is given in Fig. 3**b**. It's found that when the applied pressure was less than 1.33 kPa, the load peak current density increased approximately linearly. As the applied pressure increased to be higher than 1.33 kPa, the load peak current density increased approximately linearly too, with a smaller increasing rate. The variation tendency of the △σ was similar to that of the load peak current density, which was divided to two regions. These output behaviors are similar to the "vertical contact-separation mode triboelectric generator" [33]. The load peak current density and △σ reached ~ 0.239 μA/cm ^{2} and ~ 6.648 nC/cm ^{2}, respectively, when the applied pressure reached 6.67 kPa. By continuously increasing the applied pressure, the peak current and corresponding transferred charge density of our generator tended to be saturated, as the air bubble was completely compressed.

Furthermore, the load peak current density and △σ increased step by step under given applied pressure of 6.67 kPa and different applied frequency, from ~ 0.077 μA/cm ^{2} at 1.2 Hz to ~ 0.237 μA/cm ^{2} at 5 Hz. However, the △σ almost kept at a constant value of ~ 6.650 nC/cm ^{2} for different applied frequency (Fig. 3**c**). According to the above results, the load peak current density of the generator is related to both of the applied pressure and frequency, and the △σ is only related to applied pressure.

The output stability performance of the generator was studied by pressing and releasing for continuous ~ 90000 cycles, under given applied pressure and frequency of 6.67 kPa and 5 Hz, respectively. As indicated in Fig. 3**d**, both of the load peak current density and △σ remained at the constant values of ~ 0.245 μA/cm ^{2} and ~ 6.645 nC/cm ^{2}. This remarkable stability performance is attribute to the excellent charges capturing ability of PET electret and good flexibility and elasticity of the generator.

2.4. Stability of the flexible PET/EVA-based piezoelectret generator under harsh environments

As the megascopic electric dipoles exist inside the flexible PET/EVA-based piezoelectret generator and the electrodes are well protected, this generator has the great potential in harvesting mechanical

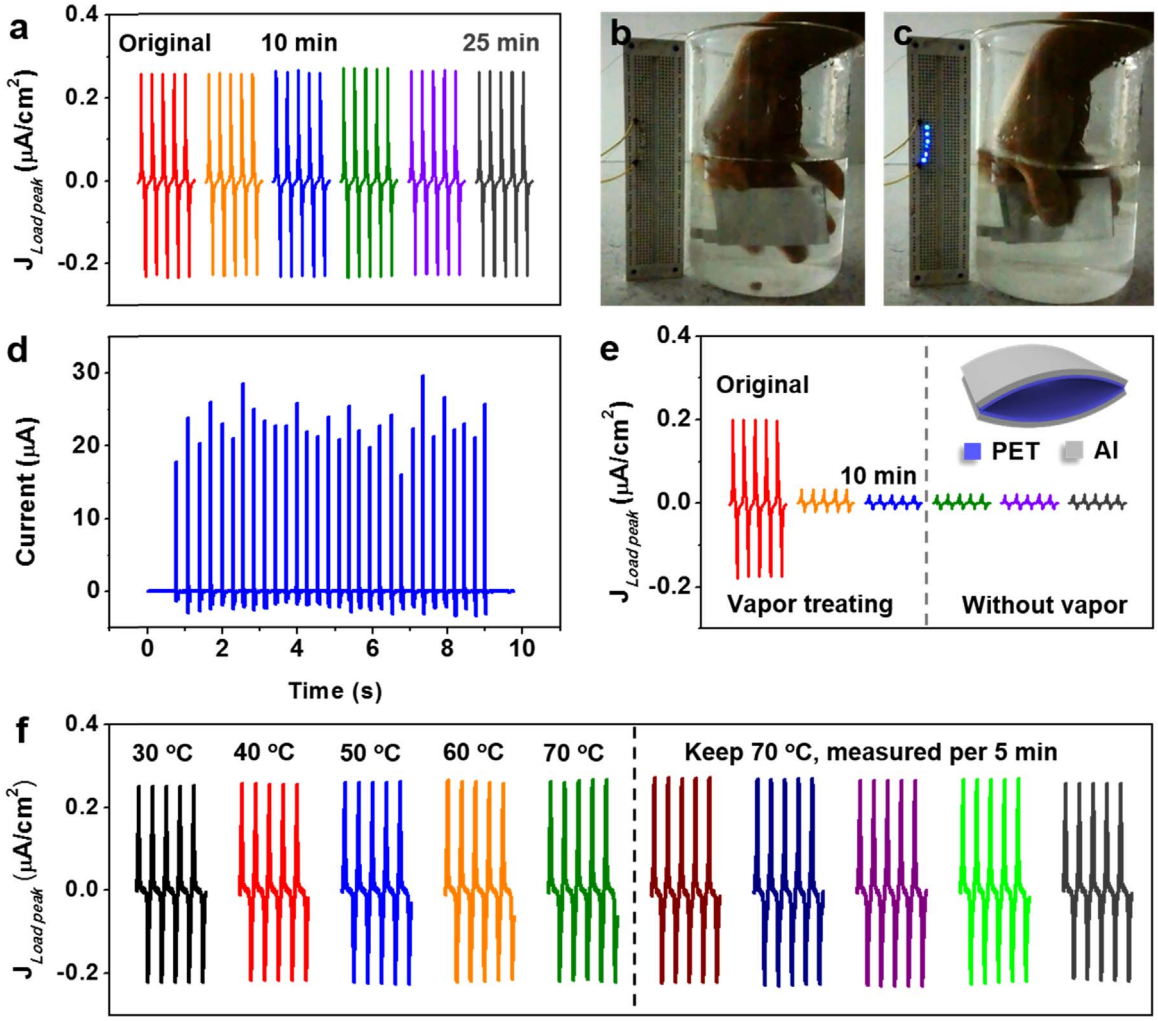

Fig. 4. Output stability characterizations of the flexible PET/EVA-based piezoelectret generator under harsh environments. (a) Current outputs of the generator under the high water vapor environment, under given applied pressure of 6.67 kPa and sinusoidal frequency of 5 Hz. Optical photos for (b) the generator under water and (c) 6 blue LEDs lit up by hand pressing the generator under water. (d) Current flowing through the LEDs when they were lit up. (e) Currents outputs for an arch-shaped generator under the high water vapor environment and the following without vapor environment, under given applied pressure and frequency of 6.67 kPa and 5 Hz. Insert in (e) showing the schematic diagram of the arch-shaped generator. (f) Current outputs for a flexible PET/EVA-based piezoelectret generator when the temperature increased form 30 ℃ to 70 ℃ and then kept at 70 ℃, under given applied pressure and frequency of 6.67 kPa and 5 Hz.

energy under harsh environments. The stability of the generator under extreme moisture environment was investigated. Specifically, the generator was placed into a closed space full of water vapor and continuously operated under given applied pressure of 6.67 kPa and sinusoidal frequency of 5 Hz, respectively (Fig. S7). Typical load current curves generated by the generator in one second were recorded for every 5 min (Fig. 4**a**). The load peak current density varied between ~ 0.256 μA/c m^2 and ~ 0.268 μA/cm ^{2} for the whole 25 min of measurement. Moreover, the generator was soaked into water (Fig. 4**b**), and 6 blue LEDs connected in series were lit up by hand pressing the generator (Fig. 4**c and Video 1**). The turn-on threshold voltage of the 6 blue LEDs was ~ 15 V (Fig. S8) and the highest peak current went through the LEDs was ~ 29.6 μA (Fig. 4**d**). Therefore, the generator generated an instantaneous output power of ~ 0.444 mW. Above results indicated that our generator had the outstanding ability in converting the mechanical energy into electricity under the extreme moisture environment or even completely immersed in water.

Supplementary material related to this article can be found online at doi:10.1016/j.nanoen.2017.05.034.

In comparison, an arch-shaped flexible generator (**insert in** Fig. 4**e**) based on PET electret film was also operated under the high water vapor environment. In this case, the surplus charges contacted with extreme moisture directly. The load peak current density dropped from ~ 0.197 μA/c m^2 to ~ 0.0185 μA/cm ^{2} after continuously operating for 10 min. Then, the generator was only operated for 3 s at each 5 min time interval after removing the vapor, the output current of the generator could not recover again (Fig. 4**e**).

The output performance of the flexible PET/EVA-based piezo-electret generator under different temperatures was characterized. A heater was used to control the temperature of the generator, which was continuously operated under the applied pressure and frequency of 6.67 kPa and 5 Hz (Fig. S9). As given in Fig. 4**f**, when the temperatures increased from 30 °C to 70 °C, the load peak current density only had relatively stable outputs between ~ 0.251 μA/c m^2 and ~ 0.263 μA/cm ^{2}. If the temperature was then kept at 70 °C for 25 min, the output currents remained stable. However, higher temperature can cause the loss of the megascopic electric dipoles inside the generator based on the short circuit TSD measurement result (Fig. 2**b**). As such, the output performance of the generator would reduce (Fig. S10).

3. Conclusions

In summary, a new type of flexible piezoelectret generator based on EVA/PET laminated film was fabricated, in which megascopic electric dipoles were captured inside the air bubble. By changing the dipole moments of the electric dipoles, the generator converted mechanical energy into electricity effectively, with d_{33} coefficient reaching ~ 6300 pC/N. Specifically, load peak current and corresponding peak power of ~ 29.6 μA and ~ 0.444 mW were reached by hand pressing the generator, and stable outputs were achieved for ~ 90000 continuous working cycles. More importantly, the generator had remarkable output stability under harsh environments with extreme moisture and temperature up to 70 °C, indicating the feasibility for wearable energy harvesting. This study provides a new, simple and efficient strategy for designing robust and reliable flexible energy harvesting devices.

Acknowledgements

This work was financially supported by the National Natural Science Foundation of China (51322210, 61434001, 51372132). Professor Liwei Lin is a core-principal investigator of Tsinghua-Berkeley Shenzhen Institute (TBSI) and we acknowledge the funding support of TBSI. The authors would like to thank facility support of the center for Nanoscale Characterization & Devices (CNCD), WNLO-HUST and the Analysis and Testing Center of Huazhong University of Science and Technology.

Appendix A. Supporting information

Supplementary data associated with this article can be found in the online version at doi:10.1016/j.nanoen.2017.05.034.

References

[1] A.D. Kuo, Science 309 (2005) 1686.
[2] C. Chang, V.H. Tran, J. Wang, Y.-K. Fuh, L. Lin, Nano Lett. 10 (2010) 726.
[3] F.-R. Fan, Z.-Q. Tian, Z.L. Wang, Nano Energy 1 (2012) 328.
[4] L. Persano, C. Dagdeviren, Y. Su, Y. Zhang, S. Girardo, D. Pisignano, Y. Huang, J.A. Rogers, Nat. Commun. 4 (2013) 1633.
[5] Y. Qi, M.C. McAlpine, Energy Environ. Sci. 3 (2010) 1275.
[6] J.M. Donelan, Q. Li, V. Naing, J.A. Hoffer, D.J. Weber, A.D. Kuo, Science 319 (2008) 807.
[7] Z.L. Wang, J. Chen, L. Lin, Energy Environ. Sci. 8 (2015) 2250.
[8] J. Yang, J. Chen, Y. Su, Q. Jing, Z. Li, F. Yi, X. Wen, Z. Wang, Z.L. Wang, Adv. Mater. 27 (2015) 1316.
[9] B.-U. Hwang, J.-H. Lee, T.Q. Trung, E. Roh, D.-I. Kim, S.-W. Kim, N.-E. Lee, ACS Nano 9 (2015) 8801.
[10] A. Ramadoss, B. Saravanakumar, S.W. Lee, Y.-S. Kim, S.J. Kim, Z.L. Wang, ACS Nano 9 (2015) 4337.
[11] H. Guo, M.-H. Yeh, Y.-C. Lai, Y. Zi, C. Wu, Z. Wen, C. Hu, Z.L. Wang, ACS Nano 10 (2016) 10580.
[12] H. Kang, H. Kim, S. Kim, H.J. Shin, S. Cheon, J.-H. Huh, D.Y. Lee, S. Lee, S.-W. Kim, J.H. Cho, Adv. Funct. Mater. 26 (2016) 7717.
[13] J. Zhong, Y. Zhang, Q. Zhong, Q. Hu, B. Hu, Z.L. Wang, J. Zhou, ACS Nano 8 (2014) 6273.
[14] J. Zhong, H. Zhu, Q. Zhong, J. Dai, W. Li, S.-H. Jang, Y. Yao, D. Henderson, Q. Hu, L. Hu, J. Zhou, ACS Nano 9 (2015) 7399.
[15] J. Zhong, Q. Zhong, G. Chen, B. Hu, S. Zhao, X. Li, N. Wu, W. Li, H. Yu, J. Zhou, Energy Environ. Sci. 9 (2016) 3085.
[16] Y.S. Ko, F.A. Nüesch, D. Damjanovic, D.M. Opris, Adv. Mater. 29 (2016) 1603813.
[17] T. Vu-Cong, C. Jean-Mistral, A. Sylvestre, Smart Mater. Struct. 22 (2013) 025012.
[18] G.M. Sessler, J. Electro. 51 (2001) 137.
[19] J. Zhong, Q. Zhong, F. Fan, Y. Zhang, S. Wang, B. Hu, Z.L. Wang, J. Zhou, Nano Energy 2 (2013) 491.
[20] Y. Yang, H. Zhang, R. Liu, X. Wen, T.-C. Hou, Z.L. Wang, Adv. Energy Mater. 3 (2013) 1563.
[21] L. Gu, N. Cui, J. Liu, Y. Zheng, S. Bai, Y. Qin, Nanoscale 7 (2015) 18049.
[22] V. Nguyen, R. Yang, Nano Energy 2 (2013) 604.
[23] H. Guo, Z. Wen, Y. Zi, M.-H. Yeh, J. Wang, L. Zhu, C. Hu, Z.L. Wang, Adv. Energy Mater. 6 (2016) 1501593.
[24] K.Y. Lee, H.-J. Yoon, T. Jiang, X. Wen, W. Seung, S.-W. Kim, Z.L. Wang, Adv. Energy Mater. 6 (2016) 1502566.
[25] S. Bauer, R. Gerhard-Multhaupt, G.M. Sessler, Phys. Today 57 (2004) 37.
[26] N. Wu, X. Cheng, Q. Zhong, J. Zhong, W. Li, B. Wang, B. Hu, J. Zhou, Adv. Funct. Mater. 25 (2015) 4788.
[27] W. Li, N. Wu, J. Zhong, Q. Zhong, S. Zhao, B. Wang, X. Cheng, S. Li, K. Liu, B. Hu, J. Zhou, Adv. Funct. Mater. 26 (2016) 1964.
[28] B. Wang, C. Liu, Y. Xiao, J. Zhong, W. Li, Y. Cheng, B. Hu, L. Huang, J. Zhou, Nano Energy 32 (2017) 42.
[29] J. Hillenbrand, G.M. Sessler, Ferroelectrics 472 (2014) 77.
[30] X. Zhang, G.M. Sessler, Y. Wang, J. Appl. Phys. 116 (2014) 074109.
[31] P. Pondrom, J. Hillenbrand, G.M. Sessler, J. Bös, T. Melz, Appl. Phys. Lett. 104 (2014) 172901.
[32] Q. Zhong, J. Zhong, X. Cheng, X. Yao, B. Wang, W. Li, N. Wu, K. Liu, B. Hu, J. Zhou, Adv. Mater. 27 (2015) 7130.
[33] L. Lin, Y. Xie, S. Wang, W. Wu, S. Niu, X. Wen, Z.L. Wang, ACS Nano 7 (2013) 8266.

Junwen Zhong is a Postdoctoral Researcher in Department of Mechanical Engineering of University of California at Berkeley, United States. He received his B.S. degree (2011) and Ph.D. degree (2016) from Huazhong University of Science and Technology, China. He majors in Flexible Generators, Wearable Electronics, Self-Powered Systems and Active Sensors.

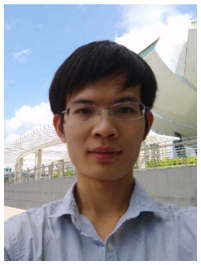

Qize Zhong received his B.E.degree in Optoelectronic Information (2011) and Ph.D. degree (2016) both from Huazhong University of Science and Technology, China. After obtained his Ph.D., he joined into Temasek laboratories @ Nanyang Technological University, Singapore as a Research Scientist. His main research is Energy Harvesting for Wearable Electronics and Self-Powered Nano- and Microsystems.

Xining Zang received her B.E. degree in Materials Science and Engineering from Shanghai Jiao Tong University in 2012. She has been pursuing her Ph.D. degree in Mechanical Engineering from UC Berkeley since 2012. Her research span from 2D materials synthesis, applications in energy storage and catalyst and 2D materials based flexible electronics.

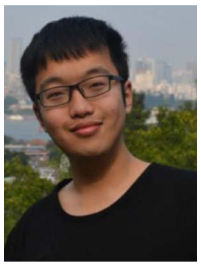

Nan Wu is a Ph.D. candidate at Wuhan National Laboratory for Optoelectronics, Huazhong University of Science and Technology. He received his Bachelor degree in Physics from Huazhong University of Science and Technology in 2014. His research interests include Piezoelectret Materials and Self-Powered Flexible Electronics.

Wenbo Li received his B. E. degree in Electronic Science and Technology from Huazhong University of Science and Technology in 2014. He is a Ph. D. candidate in Wuhan National Laboratory for Optoelectronics and School of Optical and Electronic Information at HUST. His research interests include Flexible Electronics and Piezoelectret Materials.

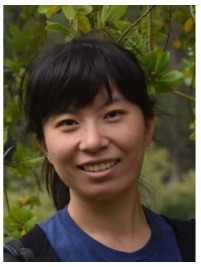

Yao Chu is a Ph.D. candidate at Sensors and Microsystems Laboratory, Tsinghua-Berkeley Shenzhen Institute. She received her B.S. degree (2014) of Mechanical Engineering from Shanghai Jiao Tong University, China and M.S. degree (2015) of Mechatronic and Robotic Systems from University of Pennsylvania, United States. Her research interests include Wearable Electronics and Paper-based Electronics.

Liwei Lin is a professor in Department of Mechanical Engineering of University of California at Berkeley, a Co-Director of Berkeley Sensor and Actuator Center (BSAC) and a Co-Deputy Director of Tsinghua Berkeley Shenzhen Institute (TBSI). He received his B. S. degree form National Tsing Hua University (Taiwan, 1986) and Ph.D. degree from University of California at Berkeley (United States, 1993). His research interests include Microelectromechanical Systems (MEMS), Nanoelect romechanical Systems (NEMS) and Nanotechnology, *etc.*